

## Brief Report

# Pathological Evidence for Residual SARS-CoV-2 in the Micrometastatic Niche of a Patient with Ovarian Cancer

Takuma Hayashi<sup>1,2,\*</sup>, Kenji Sano<sup>3</sup>, Nobuo Yaegashi<sup>2,4</sup> and Ikuo Konishi<sup>1,2,5</sup><sup>1</sup> National Hospital Organization Kyoto Medical Centre, Kyoto, Japan<sup>2</sup> The Japan Agency for Medical Research and Development (AMED), Tokyo, Japan<sup>3</sup> Shinshu University Hospital, Nagano, Japan<sup>4</sup> Department of Obstetrics and Gynecology, Tohoku University Graduate School of Medicine, Miyagi, Japan<sup>5</sup> Kyoto University Graduate School of Medicine, Kyoto, Japan

\*Corresponding author: yoyoyo224@hotmail.com

**Abstract:** In previous clinical studies, severe acute respiratory syndrome coronavirus 2 (SARS-CoV-2) infection in patients with cancer has a high risk of aggravation and mortality than in healthy infected individuals. The inoculation with the COVID-19 vaccine reduces the risk of SARS-CoV-2 infection and COVID-19 severity. However, vaccination-induced production of anti-SARS-CoV-2 antibodies is said to be lower in patients with cancer than in healthy individuals. Additionally, the rationale for why patients with cancer become more severe with COVID-19 is not well understood. Therefore, we examined the infection status of SARS-CoV-2 in primary tumor and micrometastasis tissues of patients with cancer and COVID-19. In this study, angiotensin-converting enzyme 2 (ACE2) expression was observed, and SARS-CoV-2 particles were detected in ovarian tissue cells in contact with the micrometastatic niche of high-grade serous ovarian cancer. We believe that more severe COVID-19 cases in patients with cancer may be attributed to these pathological features.

**Keywords:** SARS-CoV-2; COVID-19; micrometastatic niche; Patient with Cancer

## 1. Introduction

The World Health Organization reports that the mortality rate of patients with cancer infected with severe acute respiratory syndrome coronavirus 2 (SARS-CoV-2) is 7.6%, which is a fairly high rate compared with the 1.4% mortality rate of SARS-CoV-2-infected individuals without complications (1). The 30 day all-cause mortality was high and associated with general and cancer-specific risk factors among patients with cancer and coronavirus disease 2019 (COVID-19), with a mortality of 13.3% (1,2,3). COVID-19 severity in patients with cancer is yet to be elucidated. In patients with cancer undergoing anticancer therapy, a reduced immunity may exist (4). The pathological features of COVID-19, especially in patients with recurrent cancer or patients with cancer with relapse or metastasis, remain largely unknown. In our study, expression of angiotensin-converting enzyme 2 (ACE2), a host-side receptor for SARS-CoV-2, was observed in ovarian tissue cells in contact with the micrometastatic niche of high-grade serous ovarian cancer (HG-SOC), and SARS-CoV-2 particles were detected. Hence, we report that more severe COVID-19 cases in patients with cancer may be attributed to these pathological features.

## 2. Case Report

A 47-year-old woman was admitted to the hospital on May 18, 2022, because of trauma related to a fall. This patient reported that she had been exposed to a COVID-19 patient on May 15, 2022. Since the exposure, the patient manifested pneumonia symptoms (Supplementary Table 1). On May 15, 2022, the patient underwent a nasopharyngeal swab and was confirmed positive for SARS-CoV-2 via a reverse transcription-polymerase chain reaction (RT-PCR) test followed by treatment. She was sent home for treatment with an antipyretic and cough medicine.

At approximately 11:00 am on May 18, 2022, the patient complained of severe lower abdominal pain. The patient was examined at a nearby general hospital. Computed tomography (CT) was performed, and twisting of a left ovarian tumor with a maximum diameter of 13 cm was suspected. Because of the urgent need for surgical treatment, the patient was referred to our institution for an emergency transfer (Supplementary Table 1). After completing the transfer procedures for COVID-19 patients, the patient was taken to our hospital, which is the designated national hospital for accepting highly acute phase/tertiary critical care/COVID-19 severely ill patients, via ambulance (Supplementary Table 1).

On May 18, a chest X-ray was performed, which showed scattered ground glass-like shadows in the lower left lung field and a granular shadow in the right lung field (Supplementary Figure 1A). Sosegon Intravenous Solution 15mg, an analgesic, was administered for the lower abdominal pain and sore throat on May 18 at 10:50 pm; however, the pain persisted; hence, Acerio Intravenous Solution 1000 mg was administered (Supplementary Table 1).

On May 18, a CT scan revealed a cystic mass with a major axis of approximately 12 cm in the left ovary (Supplementary Figure 1B). The ovarian stroma was edematous. Images taken by the coronal section showed a spiral structure between the uterus and the lesion in the left ovary. The possibility of left ovarian tumor volvulus was primarily considered. A malignant ovarian tumor was suspected because a solid mass was found in the left ovarian tissue (Supplementary Figure 1B). The right ovary revealed unremarkable CT findings. Furthermore, fatty liver was also noted, but with no significant lymphadenopathy or ascites. Also, the CT findings suggested left malignant ovarian tumor pedicle torsion.

On May 19 at 01:52 am, laparoscopic left and right uterine adnexal tumor resection was performed <sup>note 1</sup> secondary to malignant left ovarian tumor torsion. The right ovary and fallopian tubes were intact. The left appendage (ovary and fallopian tube) was twisted 540° clockwise. The size of the suspected malignant ovarian tumor resembled a newborn head. Laparoscopic examination showed minimal ascites, but with no adhesions. On May 20, a decrease in blood oxygen concentration (91%) was observed while the patient was asleep; thus, oxygen inhalation was initiated with 1 L of oxygen per minut (Supplementary Table 1).

Pathological findings: To evaluate the resected ovaries and fallopian tubes, the fallopian tubes were longitudinally incised as per protocol and the fimbriated end (SEE-Fim) was extensively examined. The remaining ovaries and fallopian tubes were cut into 2–3-mm sections. Histopathological evaluation was conducted (Supplementary Figure 2). High-grade serous carcinoma was found in the papillary nodule on the right outer surface of the left ovary. Serous tubal intraepithelial carcinoma (STIC) and high-grade serous carcinoma are found in the left fimbriated end (Figure 1). No malignant findings were found in the right ovary and fallopian tube. From the immunohistochemical staining results, tumor protein 53 (TP53)-positive and Ki-67/MIB1-strongly positive highly cellular atypical and nuclear atypical cells are observed in the left fimbriated end. In the papillary nodule tissue found on the right outer surface of the left ovary, paired box gene 8 (PAX8)-positive, Wilms tumor-1 (WT-1)-positive, and TP53-diffusely strongly positive highly cellular atypical and nuclear atypical cells are observed (Figure 1, Supplementary Figure 2B).

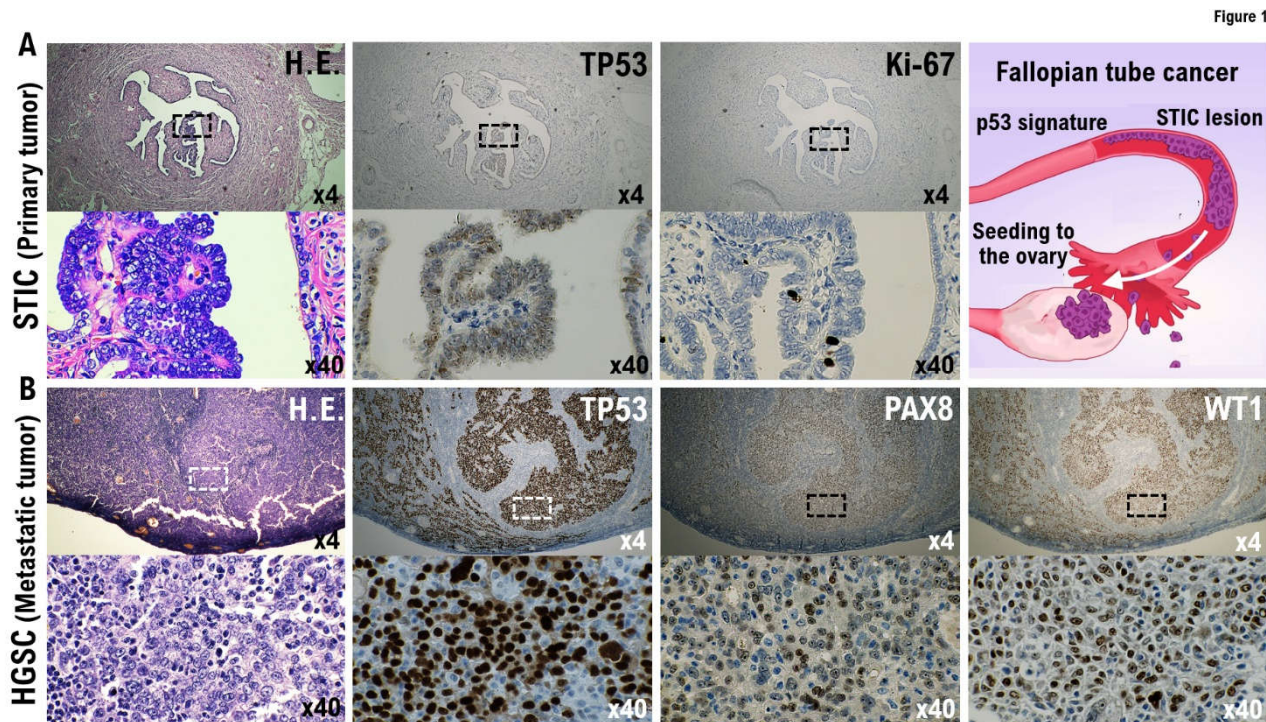


**Figure 1. Molecular pathological evidence for the development of high-grade serous ovarian cancer (HG-SOC) in a patient with COVID-19.** Molecular pathological analysis was conducted on the bilateral fallopian tubes and ovarian tissues removed from COVID-19 patients. To evaluate the resected ovaries and fallopian tubes, the fallopian tubes were longitudinally incised as per protocol and the fimbriated end (SEE-Fim) was extensively examined. The remaining ovaries and fallopian tubes were cut into 2–3 mm sections. Histopathological evaluation was conducted using these tissue sections. A. In the immunohistochemical staining results with appropriate monoclonal antibodies, TP53-positive and Ki-67/MIB1-strongly positive highly cellular atypical and nuclear atypical cells are observed in the left fimbriated end. Serous tubal intraepithelial carcinoma (STIC) and HG-SOC are found in the left fimbriated end. B. In the papillary nodule found on the right outer surface of the left ovary, PAX8-positive, WT-1-positive, and TP53-diffusely strongly positive highly cellular atypical and nuclear atypical cells are observed. High-grade serous carcinoma was found in the papillary nodule on the right outer surface of the left ovary. As shown in the panels, scales are 4× and 40×.

Previous studies have revealed that the origin of HG-SOC is STIC and/or epithelial malignancies in the fallopian tubes. STIC could be a likely precursor lesion of high-grade serous pelvic carcinomas, carcinosarcoma, and undifferentiated carcinoma with an incidence of 0.6%–7% in breast cancer 1/2 gene carriers or women with a strong family history of breast or ovarian carcinoma. Therefore, epithelial malignant cells and STICs that occur in the epithelial cell tissue of the fallopian tubes and in the fimbriated end are the primary tumors that metastasize into the ovary and form micrometastases (5,6). In forming a micrometastatic niche in multiple organs, epithelial and stromal cells in contact with circulation tumor cells (CTCs) are initialized by secretory factors from CTCs that compose the micrometastatic niche (7,8,9). ACE2 was possibly expressed in epithelial stem-like cells or progenitor cells (10,11). Also, SARS-CoV-2 infection of the epithelial cells and stromal cells in contact with or in the micrometastatic niche composed of HG-SOC found in the left ovary was considered. We investigated SARS-CoV-2 infection in the micrometastatic niche composed of HG-SOC using a molecular pathological method from the left ovarian tumor tissue resected from a COVID-19 patient.

In the immunohistochemistry (IHC) results using the anti-S100A4 antibody, which is a biomarker of HG-SOC, the cell population with a high degree of cell atypia and nuclear atypia observed in the left ovary was confirmed to be HG-SOC cells (Figure 2A). In the IHC results using anticyclin-dependent kinase 15 (CDK15) antibody, which is a

connective tissue biomarker (stroma cells), ovarian connective tissue (stroma cells) was confirmed (Figure 2A, Appendix Figure 1). A strong expression of ACE2 and cluster of differentiation 90 (CD90), which are biomarkers of stem-like cell/progenitor cell, was also observed in the ovary in some cells of the connective tissue/stroma cells in contact with or in the vicinity of the micrometastatic niche of HG-SOC (Figure 2B, Supplementary Figure 3). Conversely, ACE2 expression was not observed in the connective tissue cells (stroma cells) other than the micrometastatic niche (Figure 2B, Supplementary Figure 3). Furthermore, we conducted IHC staining using a monoclonal antibody against SARS-CoV-2 spike glycoprotein, and it was found that SARS-CoV-2 may be present in the HG-SOC tissue (Figure 2B). From IHC results using the antispike glycoprotein of SARS-CoV-2 antibody, spike protein (Spike P.) was observed in and around the cells of the connective tissue/stroma cells positive for ACE2 expression (Figure 2B, Supplementary Figure 3). Furthermore, we conducted a molecular histopathological examination using transmission electron microscopy (TEM). Consistently, images derived from observation using TEM showed clear SARS-CoV-2 particles in some cells of the connective tissue/stroma cells in contact with or in the vicinity of the micrometastatic niche of HG-SOC found in the ovary (Figure 3). As already reported (12), a heterogeneous, electron-dense, partly granular interior with ribonucleoprotein can be differentiated (Figure 3F, black arrowhead), envelope membranes of coronavirus are well resolved, and some particles show delicate surface projections (i.e., spikes; Figure 3F; white arrowhead). Thus, SARS-CoV-2 infection was confirmed in some cells of the connective tissue/stroma cells in contact with or in the vicinity of the micrometastatic niche of HG-SOC found in the ovary, and SARS-CoV-2 budding was confirmed (Figure 3). The viral particles measured 80–100 nm in diameter (Figure 3). By contrast, the expression of ACE2 and spike protein was not observed in the cortex region in the excised tissue, follicle cells, and stroma cells in tissue array sections (Supplementary Figure 4, Supplementary Figure 5).



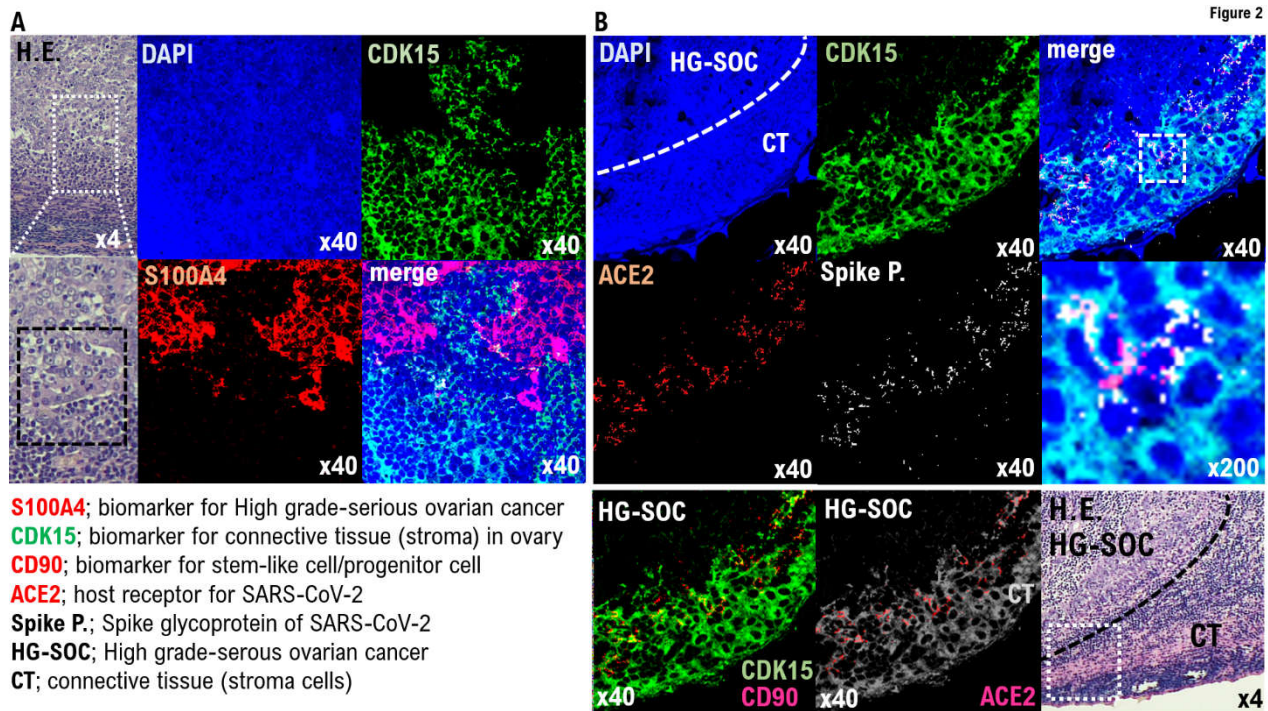


**Figure 2. SARS-CoV-2 infection in the connecting tissue in contact with or in the vicinity of HG-SOC micrometastatic niche found in the ovary.** SARS-CoV-2 infection in the micrometastatic niche composed of HG-SOC was examined through a molecular pathological method using the left ovarian tumor tissue resected from COVID-19 patients. A. From the immunohistochemistry (IHC) staining results using the anti-S100A4 antibody, which is a biomarker of HG-SOC, the cell population with a high degree of cell atypia and nuclear atypia observed in the left ovary was confirmed to be HG-SOC cells. From the IHC staining results using an anticyclin-dependent kinase 15 (CDK15) antibody, which is a connective tissue biomarker (stroma cells), the connective tissue of the ovary was markedly detected. B. A strong expression of ACE2 and CD90, which are biomarkers for stem-like cells/progenitor cells, was observed in some cells of the connecting tissue in contact with or in the vicinity of the micrometastatic niche of HG-SOC found in the left ovarian tissue. Immunohistochemistry staining was performed using a monoclonal antibody against SARS-CoV-2 spike glycoprotein. The spike glycoprotein was clearly detected, suggesting that the SARS-CoV-2 virus may be present in the HG-SOC tissue. From the IHC staining results using the antispike glycoprotein of SARS-CoV-2 monoclonal antibody, spike protein (Spike P.) was observed in and around the cells of the connecting tissue positive for ACE2 expression.

Figure 3

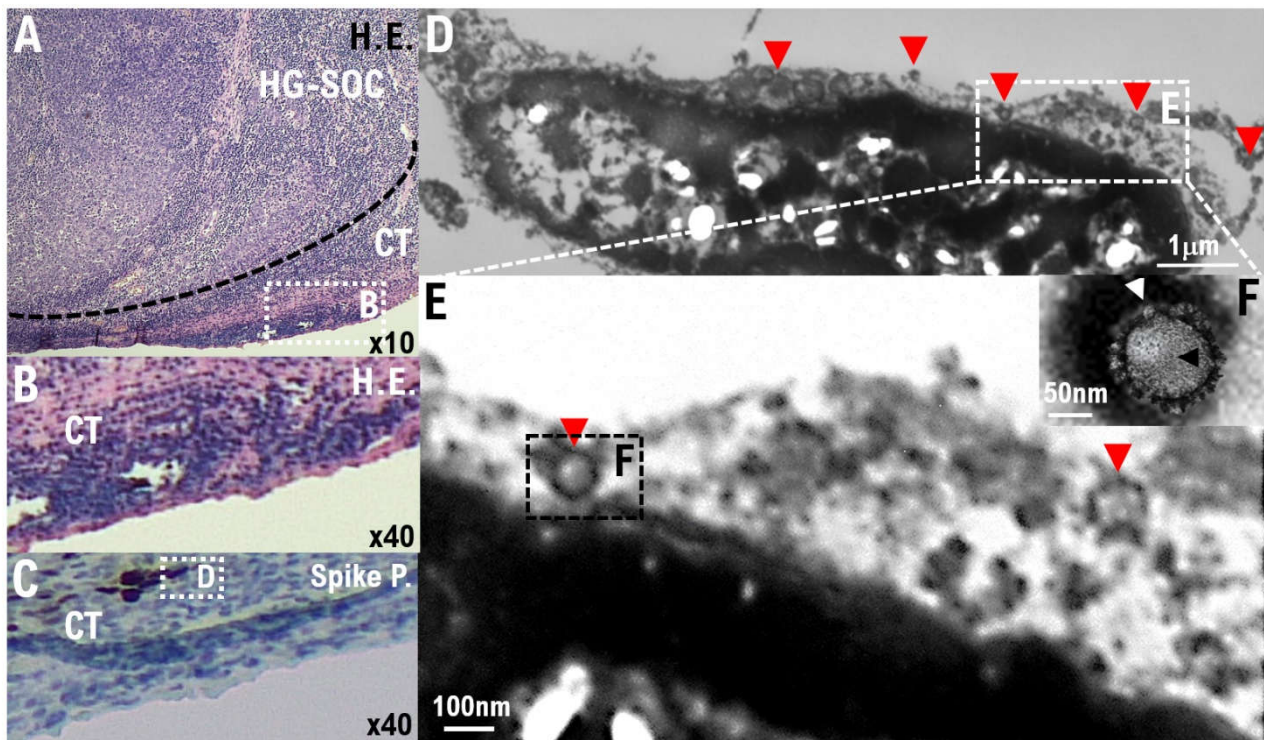


**Figure 3. SARS-CoV-2 infection of the connecting tissue in contact with or in the micrometastatic niche of HG-SOC using transmission electron microscopy (TEM).** A, B. Hematoxylin and Eosin (H.E.) staining photographs show some cells of the connecting tissue (stroma cells) in contact with or in the micrometastatic niche of HG-SOC found in the ovary. C. We conducted IHC staining using a monoclonal antibody against SARS-CoV-2 spike glycoprotein and confirmed that the spike glycoprotein of SARS-CoV-2 existed in some cells of the connecting tissue (stroma cells) in contact with or in the micrometastatic niche of HG-SOC found in the ovary. D-F. We conducted a molecular histopathological examination with TEM. Consistently, images using electron microscopic observation showed clear SARS-CoV-2 particles in some cells of the connecting tissue (stroma cells) in contact with or in the micrometastatic niche of HG-SOC found in the ovary. The findings obtained from histopathological examination using TEM indicate a heterogeneous, electron-dense, partly granular interior with a ribonucleoprotein that can be differentiated (F, black arrowhead), coronavirus envelope membranes are well resolved, and some particles show delicate surface projections (i.e., spikes; F, white arrowhead). Scales are 10000× (D), 20000× (E), and 50000× (F).

### 3. Discussion

The pathological features of COVID-19, especially in recurrent cancer tissues or metastatic tissues in patients with relapse or metastasis, remain largely unknown. In this study, a molecular pathological examination was conducted on HG-SOC excised tissue of an ovarian metastasis from a primary fallopian tube cancer from a patient with mild COVID-19 pneumonia. In the excised cancer tissue, changes in the molecular pathology were discovered, which were attributed to the SARS-CoV-2 infection. SARS-CoV-2 proliferating in the cancer tissue of patients with HG-SOC was identified through a comprehensive examination using electron microscopy and IHC staining. It should be noted that ACE2 expression was observed, and SARS-CoV-2 particles were detected in ovarian histiocytes in contact with the micrometastatic niche of HG-SOC. Factors secreted from the micrometastatic niche of HG-SOC may induce SARS-CoV-2 infection and proliferation.

A recent report demonstrated that neither coronavirus particles nor SARS-CoV-2 nucleocapsid was detected in the liver, heart, intestine, skin, and bone marrow (13). A previous study highlighted that SARS-CoV-2 remnants in the lung of a discharged COVID-19 patient after a series of nasopharyngeal swabs confirmed via RT-PCR showed negative results for SARS-CoV-2 (13). Moreover, our research results revealed that SARS-CoV-2 is



proliferating in cancer tissues in patients with cancer symptomatic of COVID-19. Therefore, compared with patients infected with COVID-19 with no comorbidities, patients with cancer and COVID-19 may have more SARS-CoV-2 proliferating in the liver, heart, intestines, skin, and bone marrow. Based on our research results, the excision of metastatic tissues in distant organs in patients with cancer and COVID-19 is considered to be an important intervention to prevent the aggravation of COVID-19.

The severity rate of patients with cancer and COVID-19 is clearly high compared with patients with COVID-19 with no underlying disorders (1). This may be attributed to the low immunity among patients with cancer; however, the exact mechanism is yet to be clarified. Our study provided pathological evidence of SARS-CoV-2 proliferation in metastatic lesions in organs of patients with cancer and COVID-19. Although surgical resection was performed in the cancerous tissue, SARS-CoV-2 proliferates in the lungs, liver, heart, intestines, skin, and bone marrow. Since clinical studies to date have shown that the third dose of the COVID-19 vaccine reduces the morbidity and mortality of COVID-19 in patients with cancer, advocating for COVID-19 vaccination to patients with cancer is necessary (14,15). Additionally, therapeutic agents such as antiviral antibody drugs should be administered to patients with cancer in the early stage of SARS-CoV-2 infection. In clinical studies, molecular pathological analysis in patients infected with COVID-19 with other cancer types is needed. Moreover, a timely follow-up of health examinations for patients with cancer is strongly recommended in clinical practice.

#### 4. Methods

**Antibodies.** The list of antibodies, which were used as the first monoclonal antibody or secondary antibody in our IHC research experiments, is shown in the Materials and Methods section in the supplementary information.

**Immunohistochemistry (IHC).** IHC staining for CD90, S100A4, ACE2, and receptor binding domain (RBD) of SARS-CoV-2 spike glycoprotein was performed on tissue sections of HG-SOC. Antibodies for CD90 (Thy1) (ab133350) and S100A4 (ab124805) were purchased from Abcam Inc. (Cambridge, UK). RBD of the spike glycoprotein was purchased from GeneTex Inc. (Irvine, CA, USA). 4',6-Diamidino-2-phenylindole (DAPI) mounting medium was purchased from VECTOR LABORATORIES, Inc. (Burlingame, CA). IHC was performed using normal methods with the primary antibody and second antibody conjugated with immunofluorescence as described previously. Details of the IHC experiment are indicated in the Materials and Methods section in the supplementary information.

**Transmission electron microscopy (TEM).** TEM was performed under a routine procedure. Tissues were fixed in 10% formaldehyde for 1 day. Briefly, specimens (approximately 1 mm × 1 mm × 1 mm in size) from each organ were fixed in 2.5% glutaraldehyde in 0.1 M phosphoric buffer (pH: 7.4) for 24 h, postfixed with 1% osmium tetroxide, dehydrated with gradient alcohol, and embedded using Eponate 12™ Kit with DMP-30 (18010, TED PELLA Inc.). Details of the IHC experiment are indicated in the Materials and Methods section in the supplementary information.

**Statistical Analysis.** All data are expressed as the mean and standard error of the mean. Normality was verified using the Shapiro–Wilk test. For comparing two groups, the unpaired two-tailed *t* test or Mann–Whitney *U* test was used. Multiple comparisons were performed using a one-way analysis of variance with a Tukey post hoc test or a Kruskal–Wallis analysis with a post hoc Steel–Dwass or Steel test. A *p*-value of <0.05 was considered statistically significant. All statistical analyses were conducted using the JMP software (SAS Institute, Cary, NC, USA).

#### Footnote

**Laparoscopic uterine adnexal tumor resection** <sup>note 1</sup>: The patient was placed in the supine position, and a 12 mm port was inserted in the navel using an open method, followed by the placement of a 5 mm port in the lower left, midline, and lower right areas of the abdomen. Surgery was performed using the diamond method. Using Enseal, we dissected the

left and right fallopian tubes, left and right pelvic funnel ligament, and mesovarium and removed the left and right adnexa (ovary and fallopian tube). After aspirating the contents of the surgical area, we placed the excised specimen in a collection bag for examination. We confirmed hemostasis, cleaned the abdominal cavity, and removed the port. The peritoneum was sutured using Vicryl 2-0, and the dermis was sutured with Mono-Dox 4-0.

**Author Contributions:** T.H. and K.S. performed most of the clinical work and coordinated the project. T.H. and K.S. conducted the diagnostic pathological studies. T.H. and S.K. conceptualized the study and wrote the manuscript. T.H., K.S., and N.Y. and carefully reviewed this manuscript and commented on the aspects of medical science. I.K. shared information on clinical medicine and oversaw the entirety of the study.

**Institutional Review Board Statement and Consent to Participate.** These experiments with human tumor tissues derived from patients with high grade-serous ovarian cancer were conducted at Shinshu University and National Hospital Organization Kyoto Medical Center in accordance with institutional guidelines (i.e., IRB approval no. M192, H31-cancer-2). The authors attended research ethics education through the Education for Research Ethics and Integrity (APRIN e-learning program (eAPRIN)). The completion numbers for the authors are AP0000151756, AP0000151757, AP0000151769, and AP000351128. Consent to participate was required as this research was considered clinical research. Subjects signed an informed consent form when they were briefed on the clinical study and agreed with content of the research.

**Data Availability Statement:** All data are shown in the manuscript figures and supplementary information. All the data generated in this study are provided in the Source Data file.

**Acknowledgments:** We appreciate David Baltimore (Nobel Laureate, California Institute of Technology) for biological comments. We thank all medical staff for providing animal care at Shinshu University School of Medicine and the National Hospital Organization Kyoto Medical Center. We appreciate Crimson Interactive Japan Co., Ltd., for revising and polishing our manuscript. This clinical research was performed with research funding from the following: Japan Society for Promoting Science for TH (Grant No. 19K09840), for KA (No. 20K16431), and START-program Japan Science and Technology Agency for TH (Grant No. STSC20001), and the National Hospital Organization Multicenter clinical study for TH (Grant No. 2019-Cancer in general-02).

**Conflicts of Interest:** The authors declare no conflict of interest.

## References

1. Kuderer NM, Choueiri TK, Shah DP, Shyr Y, Rubinstein SM, Rivera DR, et al. Clinical impact of COVID-19 on patients with cancer (CCC19): a cohort study. *Lancet*. 2020; 395: 1907-18.
2. Moris D, Tsilimigras DI, Schizas D. Cancer and COVID-19 *Lancet*. 2020; 396: 1066.
3. Kudo K, Ichihara E. COVID-19 Pneumonia *Gan To Kagaku Ryoho*. 2020 Dec;47(12):1657-61.
4. Cesaro S, Giacchino M, Fioredda F, Barone A, Battisti L, Bezzio S, et al. Guidelines on vaccinations in paediatric haematology and oncology patients. *Biomed Res Int*. 2014;2014:707691.
5. Labidi-Galy SI, Papp E, Hallberg D, Niknafs N, Adleff V, Noe M, et al. High grade serous ovarian carcinomas originate in the fallopian tube. *Nat Commun*. 2017 Oct 23;8(1):1093.
6. Ducie J, Dao F, Considine M, Olvera N, Shaw PA, Kurman RJ, et al. Molecular analysis of high-grade serous ovarian carcinoma with and without associated serous tubal intra-epithelial carcinoma. *Nat Commun*. 2017 Oct 17;8(1):990.
7. Ombrato L, Nolan E, Kurelac I, Mavousian A, Bridgeman VL, Heinze I, et al. Metastatic-niche labelling reveals parenchymal cells with stem features. *Nature*. 2019;572:603-608.
8. Hayashi T, Sano K, Aburatani H, Yaegashi N, Konishi I. Initialization of epithelial cells by tumor cells in a metastatic microenvironment. *Oncogene*. 2020 Mar;39(12):2638-2640.
9. Shiozawa Y, Pedersen EA, Havens AM, Jung Y, Mishra A, Joseph J, et al. Human prostate cancer metastases target the hematopoietic stem cell niche to establish footholds in mouse bone marrow. *J Clin Invest*. 2011;121:1298-312.
10. Salahudeen AA, Choi SS, Rustagi A, Zhu J, van Unen V, de la O SM, et al. Progenitor identification and SARS-CoV-2 infection in human distal lung organoids. *Nature* 2020;588:670-675.
11. Hayashi T, Sano K, Konishi I. Possibility of SARS-CoV-2 Infection in the Metastatic Microenvironment of Cancer. *Curr Issues Mol Biol*. 2022 Jan 5;44(1):233-241. doi: 10.3390/cimb44010017.
12. Dittmayer C, Meinhardt J, Radbruch H, Radke J, Heppner BI, Heppner FL, et al. Why misinterpretation of electron micrographs in SARS-CoV-2-infected tissue goes viral. *Lancet*. 2020 Oct 31;396(10260):e64-e65.
13. Yao XH, He ZC, Li TY, Zhang HR, Wang Y, Mou H, et al. Pathological evidence for residual SARS-CoV-2 in pulmonary tissues of a ready-for-discharge patient. *Cell Res*. 2020 Jun;30(6):541-543.



- 
14. Pinato DJ, Aguilar-Company J, Ferrante D, Hanbury G, Bower M, Salazar R, et al. On Covid study group. Outcomes of the SARS-CoV-2 omicron (B.1.1.529) variant outbreak among vaccinated and unvaccinated patients with cancer in Europe: results from the retrospective, multicentre, OnCovid registry study. *Lancet Oncol.* 2022 Jul;23(7):865-875.
  15. Khan QJ, Bivona CR, Martin GA, Zhang J, Liu B, He J, et al. Evaluation of the Durability of the Immune Humoral Response to COVID-19 Vaccines in Patients With Cancer Undergoing Treatment or Who Received a Stem Cell Transplant. *JAMA Oncol.* 2022 Jul 1;8(7):1053-1058.